Artificial neural network model for predicting load capacity of driven piles

Modelo de rede neural artificial para previsão da capacidade de carga de estacas cravadas

Modelo de red neuronal artificial para predecir la capacidad de carga de pilotes hincados

Alcineide Dutra Pessoa
ORCID: https://orcid.org/0000-0003-2598-925X
Universidade Federal do Maranhão, Brazil
E-mail: alcineidedutra@hotmail.com
Gean Carlos Lopes de Sousa
ORCID: https://orcid.org/0000-0003-0797-1099
Universidade Federal do Maranhão, Brazil
E-mail: gean_mat@yahoo.com.br
Rodrigo da Cruz de Araujo
ORCID: https://orcid.org/0000-0002-1937-3128
Universidade Federal do Maranhão, Brazil
E-mail: rodrigocruzaraujo@gmail.com
Gérson Jacques Miranda dos Anjos
ORCID: https://orcid.org/0000-0001-7260-8873
Universidade Federal do Pará, Brazil
E-mail: mirandadosanjos@gmail.comr

Abstract
In geotechnics, several models, empirical or not, have been proposed for the calculation of load capacity in deep foundations. These models run mainly through physical assumptions and construction of approximations by mathematical models. Artificial Neural Networks (ANN), in addition to other applications, are excellent computational mechanisms that, based on biological neural learning, can perform predictions and approximations of functions. In this work, an application of artificial neural networks is presented. The objective here is to propose a mathematical model based on artificial intelligence focused on Artificial Neural Network (ANN) learning capable of predicting the load capacity for driven piles. The results obtained through the neural network were compared with actual values of load capacities obtained in the field through load tests. For this quantitative comparison, the following metrics have been chosen: Pearson correlation coefficient and mean squared error. The database used to carry out the project consisted of 233 load tests, carried out in diverse cities and different countries, for which load capacity, hammer weight, hammer drop height, pile length, pile diameter and pile penetration per blow values were available. These values have been used as input values in a multilayer perceptron neural network to estimate the load capacities of the respective piles. It has been found that the proposed neural model presented, in general, correlation with field values above 90%, reaching 96% in the best result.
Keywords: Artificial neural networks; Load capacity; Deep foundations; Driven piles.

Resumo
Na geotecnia, diversos modelos, empíricos ou não, têm sido propostos para o cálculo da capacidade de carga em fundações profundas. Esses modelos funcionam principalmente por meio de suposições físicas e construção de aproximações por meio de modelos matemáticos. Redes Neurais Artificiais (RNA), além de outras aplicações, são excelentes mecanismos computacionais que, com base no aprendizado neural biológico, podem realizar previsões e aproximações de funções. Neste trabalho, é apresentada uma aplicação de redes neurais artificiais. O objetivo aqui é propor um modelo matemático baseado em inteligência artificial focado no aprendizado de Redes Neurais Artificiais (RNA) capaz de predizer a capacidade de carga de estacas cravadas. Os resultados obtidos por meio da rede neural foram comparados com valores reais de capacidades de carga obtidos em campo por meio de provas de carga. Para esta comparação quantitativa, as seguintes métricas foram escolhidas: coeficiente de correlação de Pearson e erro quadrático médio. A base de dados utilizada para a execução do estudo consistia em 233 provas de carga, realizadas em diversas cidades e diferentes países, para os quais estavam disponíveis os valores de capacidade de carga, peso do martelo, altura de queda do martelo, comprimento da estaca, diâmetro da estaca e nega. Esses valores foram usados como valores de entrada em uma rede neural do tipo perceptron multicamadas para estimar as capacidades de carga das respectivas estacas. Verificou-se que o modelo neural proposto apresentou, em geral, correlação com valores de campo acima de 90%, chegando a 96% no melhor resultado.
Palavras-chave: Redes neurais artificiais; Capacidade de carga; Fundações Profundas; Estacas cravadas.

Resumen

En geotecnia se han propuesto varios modelos, empíricos o no, para el cálculo de la capacidad de carga en cimentaciones profundas. Estos modelos se ejecutan principalmente a través de supuestos físicos y construcción de aproximaciones mediante modelos matemáticos. Las Redes Neuronales Artificiales (ANN), además de otras aplicaciones, son excelentes mecanismos computacionales que, basados en el aprendizaje neuronal biológico, pueden realizar predicciones y aproximaciones de funciones. En este trabajo se presenta una aplicación de redes neuronales artificiales. El objetivo aquí es proponer un modelo matemático basado en inteligencia artificial centrado en el aprendizaje de Redes Neuronales Artificiales (ANN) capaz de predecir la capacidad de carga de pilotes hincados. Los resultados obtenidos a través de la red neuronal se compararon con valores reales de capacidades de carga obtenidos en campo mediante pruebas de carga. Para esta comparación cuantitativa, se han elegido las siguientes métricas: coeficiente de correlación de Pearson y error cuadrático medio. La base de datos utilizada para llevar a cabo el proyecto consistió en 233 pruebas de carga, realizadas en diversas ciudades y diferentes países, para las cuales se dispuso de valores de capacidad de carga, peso del martillo, altura de caída del martillo, longitud del pilote, diámetro del pilote y penetración del pilote en el último golpe. Estos valores se han utilizado como valores de entrada en una red neuronal de perceptrón multicapa para estimar las capacidades de carga de los respectivos pilotes. Se ha encontrado que el modelo neuronal propuesto presentó, en general, correlación con valores de campo superiores al 90%, llegando al 96% en el mejor resultado.

Palabras clave: Redes neurales artificiales; Capacidad de carga; Cimentaciones profundas; Pilotes hincados.

1. Introduction

In engineering, for example, especially in geotechnics, several models, empirical or not, have been proposed for the calculation of load capacity in deep foundations. These models run mainly through physical assumptions and construction of approximations by mathematical models.

A major problem in geotechnics is the calculation of the load capacity of deep foundations (Fellenius, 2020). It is common to find in the literature several ways to perform this task, but accuracy of such solutions is, in general, imprecise, mainly due to factors such as the fact that some formulas used are obtained empirically or roughly.

Foundations are the interfacing elements responsible for carrying any buildings resting in the earth (Bowles, 1996). Cintra & Aoki (2011) define foundation as a system formed by structural elements of foundation (SEF) and the various layers of soils that surround them. It can be said, so, that foundation is the part of the construction that is responsible for receiving the loads of the structure and transmitting it to the underlying soil or rock on which it (Das, 2010; Bowles, 1996; Azeredo, 1977).

Considering its function, Bowles (1996) explains that the soil must be capable of supporting those loads without failure nor an excessive and intolerable settlement. To meet such requirements the design of foundations generally requires a knowledge of both the behavior and stress-related deformability and of geological conditions of soils that will support the foundation (Das, 2011)

Foundations are usually classified into two major categories: shallow foundations and deep foundations. The criteria for classification, although based in similar ideas, may vary according to the different authors. Das (2011, p.1) affirms that "in most shallow foundations the depth of embedment can be equal to or less than three to four times the width of the foundation". According to Bowles (1996) foundations may be classified based on where the ground the element sits: for shallow foundations, the depth is generally lower than the base dimension, while deep foundations have base length over four times its base dimension. Another classification considers that a deep foundation is one whose base rupture mechanism does not reach the surface of the ground (Hachich et al, 1998; Velloso & Lopes, 2011). In turn, NBR 6122/2010 defines that deep foundation is the foundation element that transmits the load to the ground either by tip resistance, shaft resistance, or by a combination of that two, and its tip or base is at a depth greater than twice its smallest base dimension, being at least 3.0 m (ABNT, 2010).

Focusing on the second main group, Vesic (1963) explains that deep foundations can be divided on two types: the first one refers to foundations installed by some process of excavation or drilling, not inducing significant changes in the adjacent

soil; the second one represented by foundations forced into the ground by such operations as driving, which promotes significant changes in bearing soil.

Investigation of ultimate bearing capacity of deep is fundamental (Vesic, 1963). To determine the ultimate capacity of an isolated pile, three verification mechanisms can be used: static formulas (theoretical or empirical), dynamic equations, or load tests.

Despite numerous theoretical and experimental investigation already conducted to predict the behavior and the load-bearing capacity of piles its mechanisms are not yet completely understood (Das, 2011). The same author states, then, that "the design and analysis of pile foundations may thus be considered somewhat of an art as a result of the uncertainties involved in working with some subsoil conditions" (Das, 2011, p.536).

The ultimate load capacity is obtained by the sum of the pile point capacity and the frictional resistance (skin friction) derived from the soil–pile interface (Das, 2011; Fellenius, 2020). Bowles (1996) states that although this idea is not extraordinarily complex, obtaining a prediction of capacity close to actual load tests values through its use is not a frequent event once a lack of correspondence may frequently occur due to the difficulties in determining the in-situ soil properties and its changes in the pile´s vicinity after its installation. The soil natural variability coupled with the complex pile-soil interaction, creates a difficult problem for accurate prediction (Bowles, 1996).

On the other hand, machine learning-based models have been consistently effective in predicting and functional approaches (Kalinli, Acar & Gündüz, 2011; Khanlari et al, 2012; Shahnazari & Tutunchian, 2012). Neuronal models are typically used in classification, forecasting, and other issues (Silva, Spatti & Flauzino, 2016).

The mathematical construction of Artificial Neural Networks (ANNs) is based on the electrical, chemical and biological relationships that occur in the human nervous system. In this system, the importance of neurons stands out. Neurons are excitable (or self-excitable) cells that communicate with each other by synapses, forming functional networks for processing and storing information (Haykin, 2001). The main characteristic of an ANN is the ability to "learn" tasks for which they are assigned. In addition, they can extrapolate this learning to new situations (generalization capacity). Mathematically, it can be said that the learning of an ANN consists of adjusting the set of weights to perform a specific task (Batista, 2012).

In an artificial neural network neurons are organized in the form of layers, and the way these layers are arranged defines the architecture of the network (Tian & Shang, 2006). According to Haykin (2001) the perceptron is the simplest form of a neural network initially used for classifying linearly separable patterns. This network consists of a single neuron with adjustable synaptic weights (Haykin, 2001). The Multilayer Perceptron (MLP) consists of a neural structure composed of a layer of input neurons, one or more hidden layers, and an output layer (Batista, 2012).

The most common training algorithm of a MLP is Backpropagation. This algorithm consists of using network output errors to retroactively update synaptic weights, i.e., "from output to network input" (Yan et al, 2006). The retro propagation algorithm is implemented considering two phases, forward and backward. In the forward phase the input values are multiplied by the synaptic weights in the input/output direction and at the end of that phase an error is calculated. In the backward phase, optimization techniques are applied on the error in such a way that the synaptic weights are adjusted in the output/input order (Silva, Spatti & Flauzino, 2016).

In this context, it is possible to minimize the errors and uncertainties arising from current models using neuronal models to predict load capacity of foundations, a possibility that is the main motivator of this work.

Amancio (2013) proposed a model based on perceptron-type network for predicting settlement in deep foundations. The author obtained a correlation of 0.89 as best result. Araújo, Neto & Anjos (2015) also proposed the development of a

model for predicting pile settlement using ANN. The model presented a correlation coefficient between the actual and the estimated settlements of 0.96 in the validation phase.

Erzin & Gul (2014); Padmini, Ilamparuthi & Sudheer (2008) also proposed ANN-based methodologies for predicting load capacity in deep foundations. However, what is observed in the studies is that, although all of them present a high correlation with real values, these studies do not present, for example, the values referring to internal variables of the model, which makes it difficult to be used it in practice.

The objective here is to propose a mathematical model based on artificial intelligence focused on Artificial Neural Network (ANN) learning capable of predicting the load capacity for driven piles. Unlike the studies already existing in the literature, this article presents all the internal parameters and matrices that make up the model, so that any reader can use it.

2. Methodology

As previously stated, to evaluate the quality of ultimate capacity estimates obtained the work compares the load capacity predictions obtained through ANNs models with load capacities obtained through load tests. In this article a network known as Multilayer Perceptron is used.

Considering the theoretical discussions presented by Zanella (2013), this work can be classified, in methodological terms, as to the objectives, as being explanatory and as to the procedures adopted in data collection as *ex-post facto*. Regarding the classification proposed by Pereira (2018), this research makes use of the quantitative and statistical method.

Silva et al (2010) explain that the ANN-based prediction methodology is divided into two phases: training and testing. In the training phase, part of the data is presented to the network to find the synaptic weights that minimize the errors between the network outputs and the desired values. In the test phase, the synaptic weights found in the training are used as parameters of the network and the errors are calculated.

The proposed model has been compared with real results obtained in load tests and evaluated through mean squared error and correlation between model´s outputs and field values. The database used to carry out the project then consisted of 233 load tests (Table 1), carried out in diverse cities and different countries, for which load capacity, hammer weight, hammer drop height, pile length and pile diameter values were available. The database consists of both load tests reported in the literature and monitored in the authors' professional practice. Among the 233 tests available, 153 also had information on the modulus of elasticity of the pile. For the 80 piles that did not have the exact value of such parameter, a conservative estimated value of 25GPa was adopted. Then, once this parameter is not always previously known, the proposed models have been developed under two conditions: one including the modulus of elasticity and another one that did not include such parameter.

Table 1. Load tests database.

D (m)	W (kN)	H (m)	S (mm)	L (m)	Qt (kN)	Ep (GPa)	Site
0.45	72	0.5	9	21.3	1283	36.407	Open University
0.45	72	0.5	7	6.1	698	35.339	Hattan Nacional Bank
0.45	72	0.3	1	17.4	1209	35.339	S. L. Air Force quarters
0.45	72	0.75	2	18.2	2193	34.415	S. L. Air Force quarters
0.5	72	0.75	1	8.5	1237	29.98	Voca Technology University
0.5	72	0.5	5	14.6	1519	29.98	Hemas Hospital
0.5	35	1.5	1	13.4	1924	26.297	Children's School
0.5	35	1.5	1	17.1	1832	29.045	Children's School

0.5	35	1.5	1	13.4	1924	26.297	Children's School
0.6	72	1	0.5	25.16	4671	35.154	Petroleum Head Office
0.6	72	0.75	4.5	7.1	1158	34.415	Hattan Nacional Bank
0.6	72	1	1	14.1	4495	34.415	Islamic Cultural Complex
0.6	72	1	3	23.2	3512	33.867	Laugh Property
0.6	73.5	0.75	0.2	18.61	5233	29.98	Kerawalapitiya Substation
0.6	72	1	2	17.7	2905	29.98	S. L. Air Force quarters
0.6	72	1.5	1.5	14.2	2388	29.98	S. L. Air Force quarters
0.6	72	1.5	6	20.7	2201	31.541	National Drug Laboratory
0.6	72	1.5	7	20	2467	31.541	National Drug Laboratory
0.6	72	1	12	3	2391	36.275	Nilasevena Housing Project
0.6	72	1.5	1	6.3	2690	37.224	Nilasevena Housing Project
0.6	72	1.5	1	7.7	3900	29.98	Nilasevena Housing Project
0.6	72	1.5	4	4.1	1782	29.98	Nilasevena Housing Project
0.6	73.5	0.5	0.5	21.3	2360	30.57	Melbourn Textile
0.6	35	1	1	22	2011	29.98	Melbourn Textile
0.6	35	1.25	1	21.3	2165	35.339	Melbourn Textile
0.6	35	1	1	22.1	2111	29.98	Melbourn Textile
0.6	35	1	1	24.9	2139	29.98	Melbourn Textile
0.6	35	2	2	24.66	14740	35.339	Unilever Factory
0.6	73.5	2	4.5	10.3	2950	36.09	Dambulu Furniture Piling
0.6	72	1	1	24.8	3522	27.959	Open University
0.6	72	1	1	18.3	3175	25.77	Open University
0.6	73.5	1.5	3	16.4	2800	25.08	Dental Hospital
0.6	73.5	1	1	10.5	3584	35.09	2000 Plaza-Swimming Pool
0.6	72	0.5	1	13.5	2502	29.98	Furniture Arcade Residence
0.6	72	0.5	3	12.1	1620	29.98	Furniture Arcade Residence
0.6	72	0.75	1	11.1	2375	29.98	Voca Technology University
0.6	75	0.75	5.5	18.33	1827	37.223	Advanced Technical
0.6	80	0.75	1	19.4	6027	36.08	Power Station (Kerawalapitiya)
0.6	80	0.8	0.2	27.95	4603	36.08	Power Station (Kerawalapitiya)
0.6	80	0.8	1	24.26	3023	36.08	Power Station (Kerawalapitiya)
0.7	73.5	1	1.5	23.8	2683	30.57	Melbourn Textile
0.71	73.5	1	2	20.1	3630	30.57	Melbourn Textile
0.7	73.5	1	1.5	20.3	2425	30.57	Melbourn Textile
0.7	73.5	1.5	6	10.3	2213	36.3	2001 Plaza-Swimming Pool
0.7	72	1	10	24.7	1705	29.98	Cancer Building
0.75	72	1.5	6	4.3	4060	37.607	Nilasevena Housing Project
0.75	72	3	3	15.5	3620	42.291	British Living
0.75	72	2.5	4	21.6	3294	29.98	NIBM Building
0.75	72	1.5	5	8.37	2900	34.415	Teaching Hospital
0.75	72	1.2	7.3	13.9	2675	27.498	Rotary Center
0.75	72	1.2	7	10.7	2922	27.498	Rotary Center
0.75	72	0.75	6	8.5	1464	35.339	Hattan National Bank
0.75	72	1.75	5	27.8	3706	29.98	Laugh Property

0.75	72	1.5	4	17.6	3953	29.98	S.L. Air Force quarters
0.75	72	1.5	4	14.3	3436	34.415	S.L. Air Force quarters
0.75	72	1	1	14.2	4012	35.339	S.L. Air Force quarters
0.75	72	1.75	2	18.5	4206	29.98	S.L. Air Force quarters
0.75	75	1	2	17.04	3977	34.415	Advanced Technical
0.75	75	0.75	2	16.9	2911	29.98	Advanced Technical
0.75	75	0.5	0.2	18	4526	34.415	Advanced Technical
0.75	75	0.5	2	12.9	3900	34.049	Advanced Technical
0.75	73.5	2	7.5	10.3	3184	39.19	Dambulu Furniture Piling
0.75	72	1.5	2	18.7	3455	29.98	Open University
0.75	72	1	2	9.4	4530	29.98	Voca Technology University
0.75	72	2	3	16.7	3702	29.98	Hemas Hospital
0.75	72	1.5	11.5	14.1	2781	29.98	CASA Isipatana Project
0.8	72	2.5	3	25.8	4098	30.842	Fairway Waterfrount
0.8	72	2	5	17.8	3599	29.146	Fairway Waterfrount
0.8	72	1.5	4	19.2	3804	30.1	Fairway Waterfrount
0.8	72	1.2	3	26.6	3783	34.415	Fairway Waterfrount
0.8	72	0.6	0.2	4.35	5350	34.415	Building at No. 178
0.8	72	1	13	13.8	2121	29.98	CASA Isipatana Project
0.8	75	2	7	11.1	2911	29.98	Sheraton Institute
0.8	75	2.75	2	13.1	3255	29.98	Sheraton Institute
0.8	72	2.5	9	18.2	3406	34.415	Appartment complex. at 316
0.8	72	1	1	14	4429	29.98	Furniture Arcade Residence
0.8	72	1.5	3	21.5	4429	35.339	U.K. Lanka
0.9	72	2.3	4	22.6	4862	30.1	Open University
0.9	72	1.5	3	9.61	3881	34.415	Teaching Hospital
0.9	72	1.75	3	14.4	5263	34.415	S.L. Air Force quarters
0.9	72	1.5	1	22.9	9737	34.415	H.O. Building for Costoms
0.9	72	1.5	1.5	19	5025	34.415	H.O. Building for Costoms
0.9	72	1.5	0.5	17.8	10389	34.415	H.O. Building for Costoms
0.9	72	1.75	3	20.7	5150	34.415	H.O. Building for Costoms
0.9	72	1.5	4	13.2	3845	27.596	Rotary Center
0.9	72	1	1	5.1	9944	34.415	Sri-Ja-pura University
0.9	72	2.5	3	15.1	4076	29.98	Hemas Hospital
0.9	72	1.5	3.2	19.4	4089	36.087	Medical ward complex
0.9	72	1	0.1	25.7	5037	39.059	Petroleum Head Office
0.9	80	2	0.5	16.8	11124	36.08	Power Station (Kerawalapitiya)
0.9	80	2	0.5	16.9	12324	36.08	Power Station (Kerawalapitiya)
1	72	2.5	5	21.7	5938	29.98	Fairway Waterfrount
1	72	2	10	15.5	5949	34.415	Fairway Waterfrount
1	72	2.2	9.5	23.4	5901	34.415	Fairway Waterfrount
1	72	2	2	28.35	6857	34.415	Petroleum Head Office
1	72	2.5	2.5	22.5	7805	34.968	Iceland Residencies
1	73.5	1.1	0.5	18.6	7141	34	Apartment Develop Project
1	73.5	1.5	8	25.33	4100	29.98	Grand Metropoliton

1	73.5	1.75	1.5	28.1	11790	37.224	Grand Metropoliton
1	73.5	1.5	1	29	12155	33.504	Grand Metropoliton
1	72	1.5	11	15.9	4964	34.599	H.O. Building for Costoms
1	72	2	2	22.1	4915	34.415	H.O. Building for Costoms
1	72	1.75	0.5	20.6	7348	31.541	H.O. Building for Costoms
1	72	1.5	0.1	24.7	7405	29.98	Flyover Bridge (Kelaniya)
1	72	1.5	0.2	26.4	7041	31.016	Flyover Bridge (Kelaniya)
1	72	1	1	20.8	5832	29.98	Flyover Bridge (Kelaniya)
1	72	1.5	3	24.4	4150	29.298	Flyover Bridge (Kelaniya)
1	75	1.5	0.8	9.8	4280	34.415	Elevated Water tanks
1	75	1.5	2	10.8	4462	34.415	Elevated Water tanks
1	75	2	2	10	3246	37.033	Elevated Water tanks
1	75	1.5	2.5	10.3	3416	36.275	Elevated Water tanks
1	75	1	3	10.02	3873	36.275	Elevated Water tanks
1	75	1	5	9.3	3279	36.275	Elevated Water tanks
1	72	1.5	1	19.48	3250	34.415	Flyover Bridge (Nugegoda)
1	72	2	2.5	25.17	3742	41.139	Flyover Bridge (Nugegoda)
1.2	75	2.5	2.5	24.8	11149	23.519	Iceland Residencies
1.2	75	2.5	0.5	23.9	11350	27.465	Iceland Residencies
1.2	72	1.5	0.5	26	10480	34.415	H.O. Building for Costoms
1.2	72	2	2	21.7	7142	34.415	H.O. Building for Costoms
1.2	72	2	1	22	8530	34.415	H.O. Building for Costoms
1.2	72	2	3	19.6	6852	35.339	Medical ward complex
1.2	72	1.5	0.1	23.2	8127	29.894	Flyover Bridge (Kelaniya)
1.2	72	2	1	23.2	6380	34.415	Flyover Bridge (Kelaniya)
1.2	72	2	2	20.4	5991	41.542	Flyover Bridge (Nugegoda)
1.2	85	1.5	1	8.9	8800	34.415	Apartment Complexes
1.2	72	3	2	21.1	8710	37.223	Central Hospital
1.8	200	2.285	4	22.7	17516	39.157	Mayfair City
1.8	200	2.5	1	19	21923	42.945	Mayfair City
1.8	200	2.3	3	20.95	17660	39.157	Mayfair City
1.8	200	2.5	5.5	23	15918	32.604	Mayfair City
0.2	13	0.993	1	11	928	39.157	Housing complexes
0.2	13	0.397	1	23	564	39.157	Housing complexes
0.2	13	0.523	1	11.1	876	39.1571	Housing complexes
0.2	13	1.223	1	31.6	934	34.4151	Housing complexes
0.2	13	1.14	1	18.2	1299	34.4151	Housing complexes
0.2	13	0.91	20	37	387	42.149	Housing complexes
0.2	13	1.108	20	37	311	44.2047	Housing complexes
0.35	25	0.815	0.9	13.3	2184	31.893	Laboratory Complex
0.35	25	0.951	3	10.3	1276	31.893	Laboratory Complex
0.4	25	1.158	1.8	11.1	1610	39.157	Arogya Hospital
0.3	20	1.5	0.5	19.25	1482	36.08	Kalmuni-Ampara
0.3	20	1.5	0.2	19	1231	36.08	Kalmuni-Ampara
0.3	50	0.5	1	19	1557	36.08	Kalmuni-Ampara

0.3	50	0.5	0.5	19	1589	36.08	Kalmuni-Ampara
0.3	30	1	0.5	19.5	1630	36.08	Kalmuni-Ampara
0.3	30	1	0.2	19.1	1905	36.08	Kalmuni-Ampara
0.3	30	1	0.5	16.25	1508	36.08	Kalmuni-Ampara
0.35	35	0.45	3	6	920	30.57	Factory Building
0.35	35	0.5	1	6.1	1530	30.57	Factory Building
0.355	30	1	1	12	1508	36.08	Water Supply Project
0.355	30	1	0.5	15	1879	36.08	Water Supply Project
0.355	50	1	0.5	15	961	36.08	Canal Road Project
0.4	32	1.6	0.2	24	2432	36.08	VIBC Hall
0.38	50	1.2	23	30.4	1880	25	Rio de Janeiro - RJ
0.38	50	1	13	30.9	2160	25	Rio de Janeiro - RJ
0.38	50	1.2	7	32.2	2320	25	Rio de Janeiro - RJ
0.42	42	1.6	7	26.8	1512	25	Rio de Janeiro - RJ
0.5	50	2	26	32	2580	25	Rio de Janeiro - RJ
0.38	50	0.6	3	28.6	2006	25	Rio de Janeiro - RJ
0.42	50	1.5	3	31.9	2600	25	Rio de Janeiro - RJ
0.6	50	2.6	6	34.3	4290	25	Rio de Janeiro - RJ
0.5	50	1.8	5	31.7	3200	25	Rio de Janeiro - RJ
0.6	50	2.2	6	31.9	3210	25	Rio de Janeiro - RJ
0.6	70	1.6	5	27.7	2900	25	Rio de Janeiro - RJ
0.5	70	1.4	5	31.3	4280	25	Rio de Janeiro - RJ
0.5	50	1.8	3	24.8	3450	25	Rio de Janeiro - RJ
0.7	70	1.6	8	26.3	3168	25	Rio de Janeiro - RJ
0.5	70	1.2	3	22.8	3220	25	Rio de Janeiro - RJ
0.7	70	1.6	2	23	3256	25	Rio de Janeiro - RJ
0.38	50	1.2	3	23	1900	25	Rio de Janeiro - RJ
0.6	50	2.5	5	26.4	4370	25	Rio de Janeiro - RJ
0.7	70	1.5	5	30.1	3850	25	Rio de Janeiro - RJ
0.38	70	0.6	2	31.1	1955	25	Rio de Janeiro - RJ
0.5	50	1.2	4	32.9	3200	25	Rio de Janeiro - RJ
0.42	50	1.2	2	29.2	2048	25	Rio de Janeiro - RJ
0.5	70	1.5	4	30.2	2190	25	Rio de Janeiro - RJ
0.6	70	2	3	26.3	4100	25	Rio de Janeiro - RJ
0.5	70	1.2	5	26.8	2750	25	Rio de Janeiro - RJ
0.6	50	2.4	3	22.2	2800	25	Rio de Janeiro - RJ
0.38	50	1.5	5	22.7	1500	25	Rio de Janeiro - RJ
0.38	50	1.5	3	40	2660	25	Rio de Janeiro - RJ
0.5	50	1.6	5	30	2950	25	Rio de Janeiro - RJ
0.5	50	1.5	3	29.1	3580	25	Rio de Janeiro - RJ
0.5	70	1.2	5	35.2	2800	25	Rio de Janeiro - RJ
0.26	50	0.4	20	18.9	700	25	Cubatão-SP
0.26	50	0.4	10	21.12	960	25	Cubatão-SP
0.26	18	1	0.6	10.5	450	25	Sumaré-SP
0.26	18	1	10	11.2	450	25	Sumaré-SP

0.26	20	0.6	0.6	9.25	600	25	Jaguaré-SP
0.26	22	0.7	0.4	3.3	600	25	Via Anhanguera - SP
0.33	50	0.5	10	21.1	1000	25	Cubatão-SP
0.33	50	0.6	20	39.9	800	25	Santos-SP
0.33	25	0.7	0.7	9.9	600	25	Via Anhanguera - SP
0.33	22	0.7	0.9	11.5	720	25	S. Bernardo do Campo-SP
0.33	25	1	15	23	900	25	Santa Cruz-RJ
0.42	50	0.8	1	21.35	1950	25	S. Sebastião-SP
0.42	50	1	15	12	1350	25	Volta Redonda-RJ
0.42	35	1.5	0.3	9.7	1350	25	S. Caetano do Sul-SP
0.42	50	1	0.3	21.15	1050	25	Duque de Caias-RJ
0.42	38	1	10	14.97	980	25	Sumaré-SP
0.42	50	1	40	23.15	1350	25	Santa Cruz-RJ
0.5	50	1	15	23	1915	25	Caju-RJ
0.5	50	1	18	21.8	1500	25	S. José dos Campos-SP
0.5	35	2	48	18	2000	25	Angra dos Reis-RJ
0.5	35	2	50	15.4	2140	25	Angra dos Reis-RJ
0.5	35	2	35	13.1	2200	25	Angra dos Reis-RJ
0.5	50	1	15	15.8	1560	25	Duque de Caias-RJ
0.5	70	1.2	10	26.5	1800	25	Santos-SP
0.5	70	1.2	25	34	1800	25	Santos-SP
0.5	70	1.2	20	34	1800	25	Santos-SP
0.5	40	1	20	14	1950	25	Ipatinga-MG
0.5	65	1	30	29.5	1950	25	Santa Cruz-RJ
0.5	50	1	15	27.4	1950	25	Santa Cruz-RJ
0.5	50	1	20	38.85	1950	25	Santa Cruz-RJ
0.5	65	1	20	28.75	1950	25	Santa Cruz-RJ
0.5	35	2	0.5	26.4	2100	25	Barueri-SP
0.5	46.1	1	0.9	19.9	2100	25	Barueri-SP
0.5	52.7	1	0.9	16.5	2100	25	Barueri-SP
0.5	50	1	0.9	20.2	2100	25	Barueri-SP
0.5	35	2	20	9.4	2100	25	Barueri-SP
0.5	35	2	10	18.7	2100	25	Barueri-SP
0.5	35	2	7	28.4	1950	25	S. Caetano do Sul-SP
0.5	35	1.8	30	11.7	2600	25	Barcarena-PA
0.6	45	2	10	9.3	2550	25	Duque de Caxias – RJ
0.6	35	2	26	21.4	2920	25	Duque de Caxias -RJ
0.6	63	1.2	10	29.8	2660	25	Duque de Caias-RJ
0.6	45	2	14	27.1	2800	25	Santa Cruz -RJ
0.6	63	1	22	28.7	3500	25	Av. dos Autonomistas – SP
0.6	45	2	15	29	2550	25	Av. dos Autonomistas – SP
0.6	35	2	15	35.5	2550	25	Santa Cruz – RJ
0.6	35	1.8	10	21.25	2550	25	-
0.7	45	2	10	30.1	3450	25	São Paulo – SP

Source: Adapted from Lobo (2005), Jayaweera (2009) and SCAC (2013).

The variables hammer weight (W), hammer drop height (H), pile length (L), pile diameter (D), modulus of elasticity (Ep) and the permanent penetration of a pile caused by the application of the last hammer blow (S) have been used as inputs values in a multilayer perceptron neural network to estimate their load capacity. In each training of the neural network were used percentages of 70% to 80% of the data, with the rest being left to test / validation of the topology. The results obtained, as well as the topology of the networks and their parameters will be presented in graphs and tables.

To evaluate the quality of the predictions made by the proposed model, the results obtained have been compared with the actual results obtained through load tests. For this quantitative comparison, the following metrics have been chosen: Pearson correlation coefficient and mean squared error.

Correlation identifies two groups of data with some relationship to each other, that is, if high (low) values of one of the variables implicated in high (or low) values of another variable. A correlation analysis provides a number that summarizes the degree of linear relationship between the two variables, which is called the correlation coefficient. The choice of the correlation coefficient (Equation 1) was because it is a metric widely used to evaluate comparisons such as the one this research wants to make (Benesty et al,2009).

$$\rho = \frac{Cov(X,Y)}{\sqrt{Var(X)Var(Y)}}$$

(1)

where *X* and *Y* are the compared variables.

However, the linear correlation coefficient may lead to false conclusions when used in as an accuracy index of predictions or simulations. For example, simulated and observed values can be highly correlated, even in situations where simulations are overestimating or underestimating what is observed.

Thus, a measure often used to evaluate the accuracy of numerical models is the Mean Squared Error (MSE). The MSE is defined as the mean of the difference between the estimator value and the squared parameter.

The mean squared error is obtained by the expression presented in Equation 2 (Willmott & Matsuura, 2005).

$$MSE = \frac{\sum_{i=1}^{n}(y - \hat{y})^2}{n}$$

(2)

where y is the measured value, $\hat{y}$ is the value obtained in the analyzed model and n is the number of samples.

In other words, the choice of correlation was because this is widely used to evaluate comparisons of this type, while the use of the mean squared error is important because its a better way to verify the accuracy of the model.

All simulations have been made by fixing the network topology in only one hidden layer and with sigmoid activation function. In some cases, the learning rate and the number of neurons of the hidden layer (nno) have been varied. The learning rate μ is a parameter that defines, mainly, the distance between the network output error and the minimum error that the problem admits. The number of neurons in each layer defines the nonlinearity of the data presented to the network. It is worth

remembering that the values chosen for such parameters are chosen empirically, which justifies the performance of several tests to verify which parameters best fit the problem under analysis.

In the simulations performed the number of neurons in the input layer has always been equal to the number of inputs and in the output only one neuron has been considered. From the total set of data, 202 values have been randomly chosen for network training and 30 for testing.

3. Results and Discussion

First models were tested using hammer weight, hammer drop height, pile length, pile diameter and permanent penetration per blow values as parameters, without including modulus of elasticity. The comparison of ANN results and load tests are presented in figures. Optimal weights obtained in each simulation are also presented.

For a better understanding of the importance of weight matrices it is necessary to be in mind that the columns of w1, for example, refer to coefficient vectors of each input variable ordered as follows: hammer weight (W), hammer drop height (H), pile length (L), pile diameter (D), permanent penetration of the pile caused by the application of the last hammer blow (S) and bias (characteristic value of RNA models).

The comparison of ANN results (when the learning rate μ=0.1000 and nno=8 was used) with the actual measured values is shown in Figure 1. On this first attempt the MSE obtained was 2.0689×10^6 and the correlation achieved 0.9415.

Figure 1. Comparison between actual values and ANN outputs (not including modulus of elasticity, $\mu = 0.1000$ and $nno = 8$).
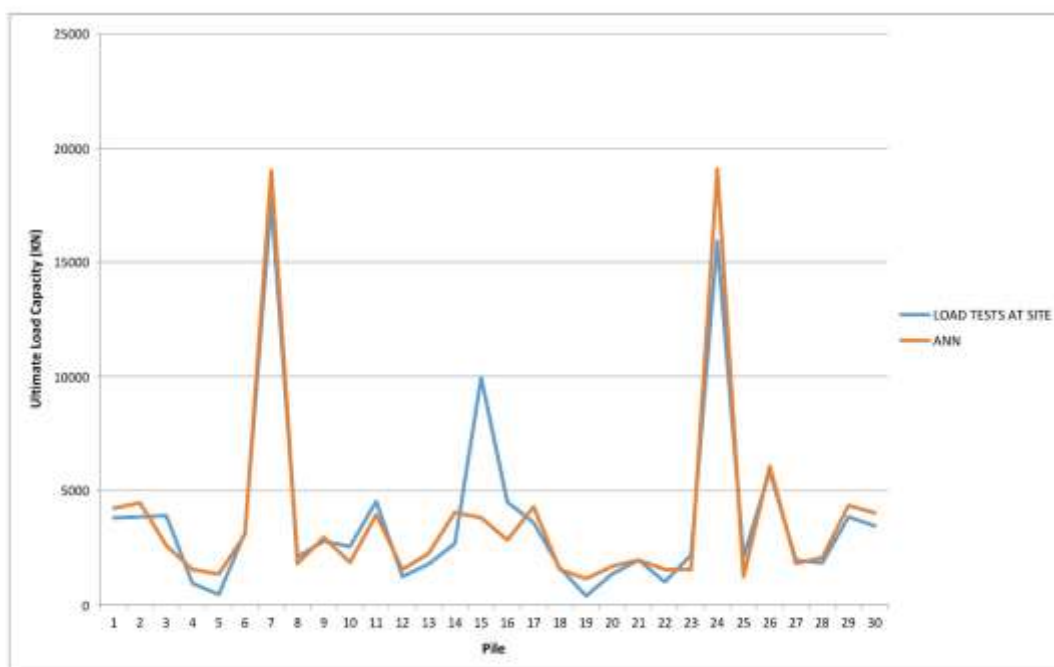
Source: Authors.

Analyzing Figure 1 it can be noticed that the network obtained an excellent approximation of the values, except for sample 15, which showed a significant difference between the actual and estimated values.

The optimal weights obtained in this simulation were:

$$w1 = \begin{bmatrix} 1.08 & 0.78 & 0.82 & 0.48 & -0.26 & 0.31 \\ 0.49 & 0.75 & 0.60 & 0.38 & 0.63 & 0.09 \\ 0.89 & 0.65 & 0.75 & -0.16 & 0.16 & 0.62 \\ 1.23 & 1.07 & 0.95 & -0.22 & 0.45 & 0.15 \\ 0.50 & 0.66 & 0.37 & 0.82 & 0.85 & 0.46 \\ 0.80 & 1.21 & 0.26 & 0.50 & -0.77 & 0.35 \\ 0.32 & 0.39 & 0.31 & 0.78 & 0.75 & 0.42 \\ -0.13 & 0.30 & 0.79 & 0.99 & 0.86 & 0.65 \end{bmatrix}$$

and

$$w2 = \begin{bmatrix} 1.40 & 1.09 & -0.10 & 0.78 & 0.88 & -0.03 & 1.34 & -0.40 & -0.72 \end{bmatrix},$$

where w1 is always the matrix of hidden layer weights and w2 always the output layer weight matrix.

The weights obtained in the first simulation indicate that the variables whose coefficient values contribute most in absolute terms are: hammer weight (W) and hammer drop height (H) (first and second column of w1 respectively).

Figure 2 graphically presents the comparison obtained when the learning rate μ=0.5000 and nno=8 were used. In this case, there was an improvement in the MSE result (1.4357×10^6) and a worsening in the correlation (0.7849).

Figure 2. Comparison between actual values and ANN outputs (not including modulus of elasticity, $\mu = 0.5000$ and $nno = 8$).
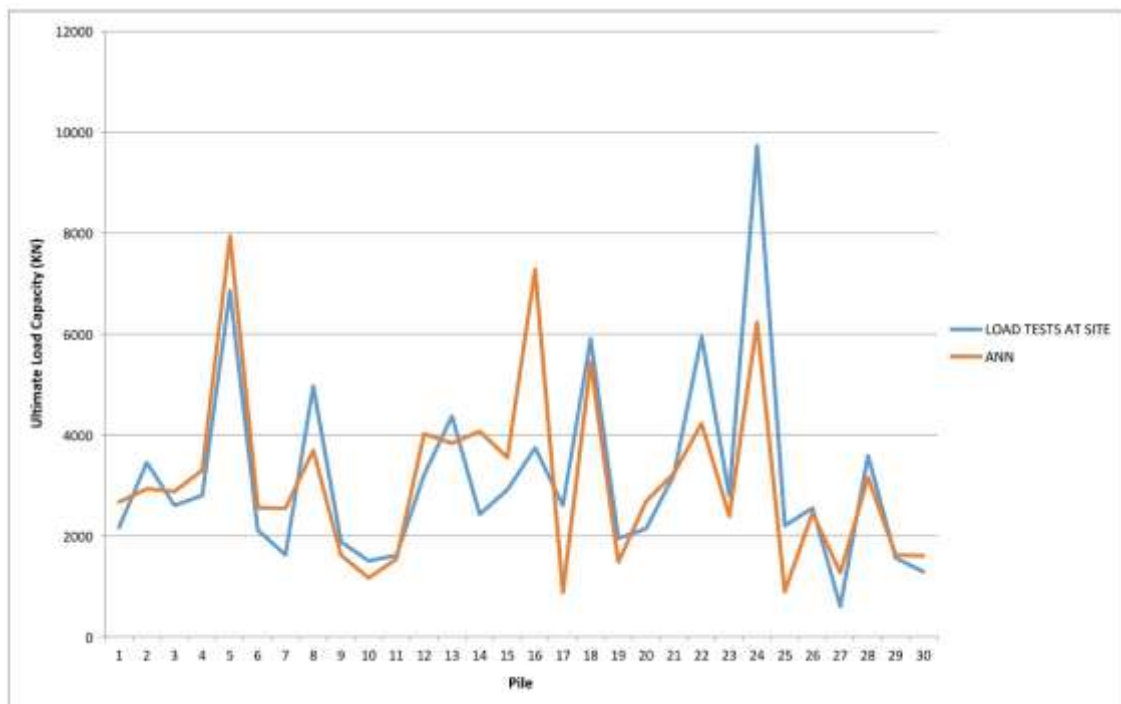
Source: Authors.

In the second simulation, the greatest discrepancies between the actual values and those observed at the network output were observed for samples 22 and 24. For the other samples the network made a good prediction.

The optimal weights obtained in this simulation were:

$$w1 = \begin{bmatrix} 1,16 & 0.72 & 0.65 & 0.0 & -0.4 & 0.87 \\ 0,0 & -0.4 & -0.2 & 0.65 & 2.02 & 0.67 \\ 0,39 & 0.96 & 0.68 & 0.55 & 0.11 & 0.20 \\ 1.03 & 0.73 & 0.23 & 0.72 & 0.23 & 0.56 \\ 0.45 & 0.24 & 0.63 & 0.72 & 0.90 & 0.90 \\ 0.29 & 0.85 & 0.11 & 0.77 & 0.83 & 0.06 \\ 1.25 & 0.59 & 0.81 & 0.18 & -0.6 & 0.68 \\ 0.31 & 0.66 & 0.42 & 0.94 & -0.5 & 0.15 \end{bmatrix}$$

and

$$w2 = \begin{bmatrix} 1.56 & 1.03 & -1.51 & 0.64 & 0.37 & -0.17 & 0.07 & 1.02 & 1.01 \end{bmatrix},$$

with w1 and w2 having the same meanings described in the previous case.

For the second simulation, the columns of the w1 weight matrix suggest that the values referring to the hammer weight coefficients, on average, had a greater contribution to the model obtained.

The result of comparisons when the learning rate $\mu=0.9000$ and nno=8 were used is shown in Figure 3. In this case the MSE was much worse than the values obtained in the previous two attempts, reaching 5.4141×10^6 while the correlation remained close to that of the second test, reaching 0.7758.

Figure 3. Comparison between actual values and ANN outputs ($\mu = 0.9000$ and $nno = 8$).
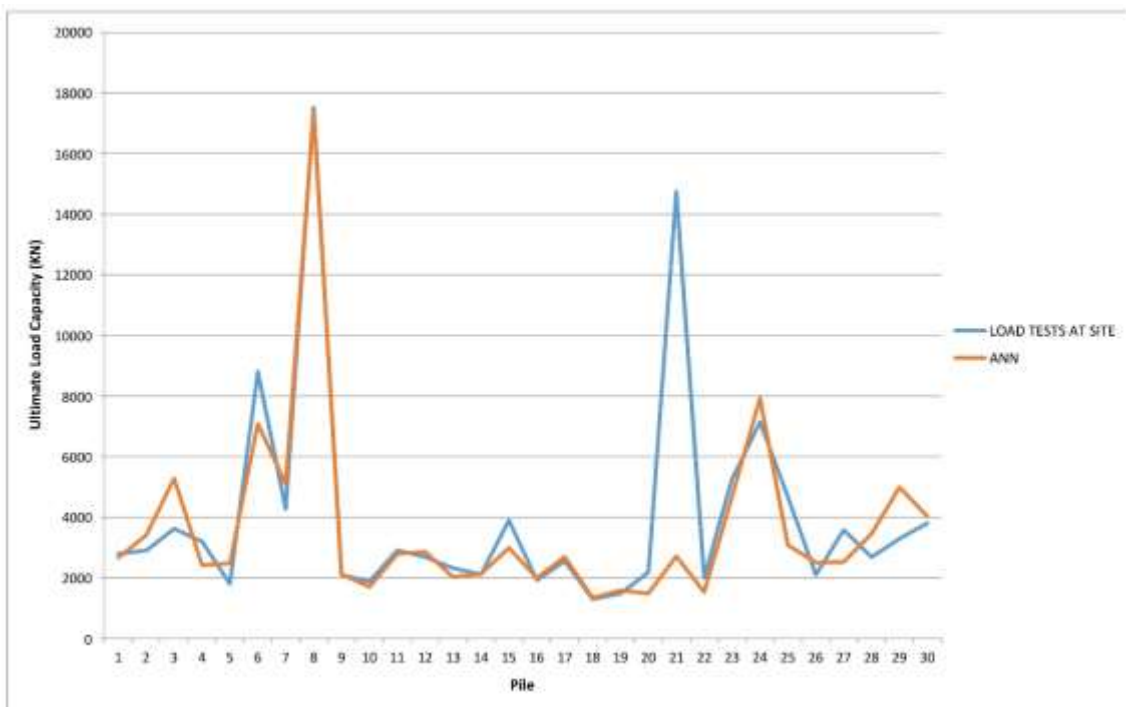
Source: Authors.

Observing Figure 3, it may be highlighted that although the neural model performed good approximations, in one of the samples (number 21), the difference between the value of the measured load capacity and the network output is visibly unacceptable.

The optimal weights obtained in this simulation were:

$$w1 = \begin{bmatrix} 0.44 & 0.47 & 0.14 & 0.12 & 0.71 & 0.32 \\ 0.32 & 0.36 & 0.53 & 0.61 & 1.07 & 0.86 \\ 0.98 & 1.02 & 0.69 & 0.50 & -0.1 & 0.16 \\ 0.35 & 0.96 & 0.36 & 0.36 & 0.96 & 0.68 \\ 0.13 & 0.96 & 0.63 & 0.80 & 0.07 & 0.48 \\ 1.13 & 1.19 & 1.10 & 0.04 & -0.3 & 0.21 \\ 0.61 & 0.40 & 0.36 & 0.44 & 0.45 & 0.70 \\ 0.86 & 0.32 & 0.45 & 0.87 & 0.13 & 0.45 \end{bmatrix}$$

and

$$w2 = \begin{bmatrix} 1.67 & -0.06 & -0.47 & 0.95 & -0.15 & -0.08 & 1.58 & 0.37 & 0.48 \end{bmatrix},$$

Observing the weight matrices of the third simulation, a certain homogeneity is perceived in the relationship between the vectors that compose the coefficients, but as in first simulation the variables hammer weight (W) and hammer fall height (H) present a superiority in the values of their coefficients.

In the following simulations the Modulus of Elasticity of the pile (in KN/m²) was introduced to the ANN input set. The results obtained when using the learning rate $\mu=0.1000$ and nno=2 are shown in Figure 4. In this simulation the MSE was 2.8504x10^6 and the correlation 0.9005.

Figure 4. Comparison between actual values and ANN outputs (including modulus of elasticity, $\mu = 0.1000$ and $nno = 2$).
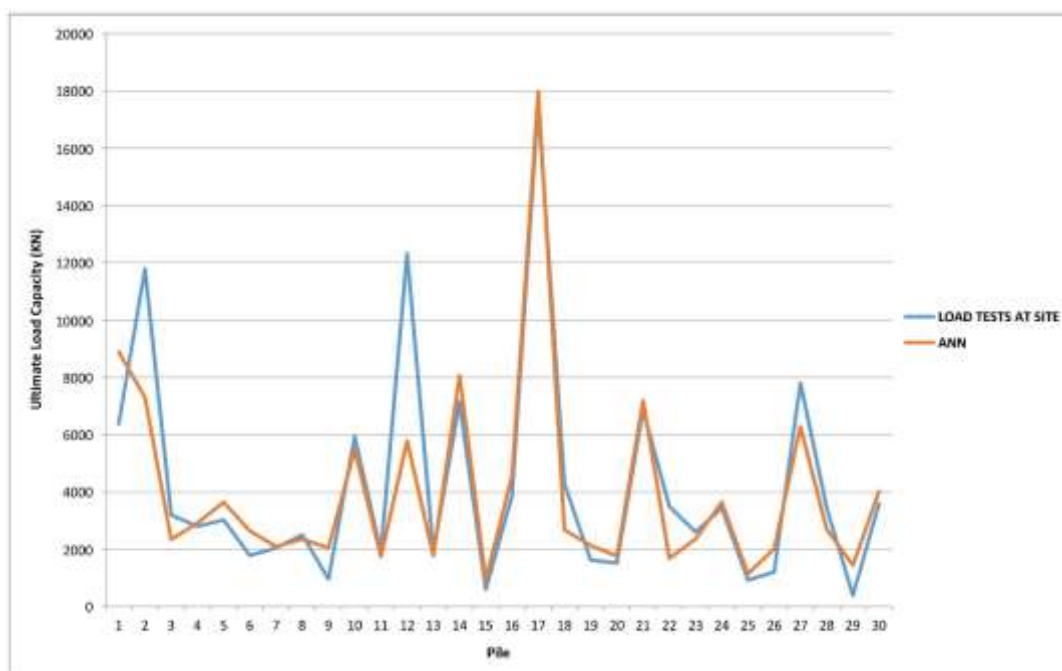
Source: Authors.

The pattern verified in figures 1 to 3 is repeated when we observe Figure 4, that is, the neural network performs, in general, good approximations, but for some isolated samples the performance is unsatisfactory. In this simulation, in particular, the network fails to approach samples 2 and 12.

The optimal weights obtained in this simulation were:

$$w1 = \begin{bmatrix} 1.62 & 1.38 & 0.60 & -0.06 & -2.54 & 0.59 & -0.14 \\ 0.57 & 1.67 & 0.71 & 1.14 & 0.00 & 0.05 & 0.63 \end{bmatrix}$$

and

$$w2 = \begin{bmatrix} 2.39 & 2.63 & 1.40 \end{bmatrix},$$

The w1 weight matrix of the fourth simulation indicates that the second column has, on average, a higher value than the other ones, indicating once again the variable hammer drop height is, in fact, an important information in the prediction of load capacity.

Figure 5 presents the comparison results when the learning rate μ=0.9000 and nno=4 were used. The MSE obtained in this simulation decreased to 0.8602×10^6 while the correlation rose to 0.9637.

Figure 5. Comparison between actual values and ANN outputs ($\mu = 0.9000$ and $nno = 4$).
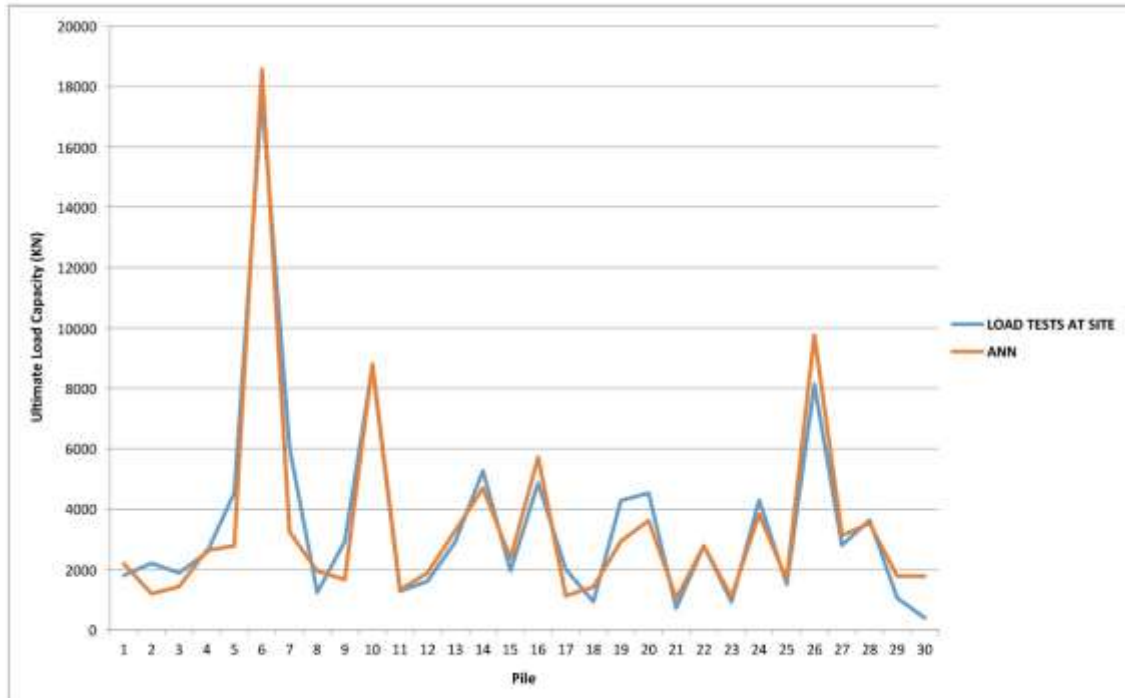
Source: Authors.

In Figure 5, the results presented demonstrate the best network performance among the simulations performed. In this figure, it is perceived that the approximation is well performed by the model for all samples, and this fact is ratified with the correlation and error values mentioned above.

The optimal weights obtained in this simulation were:

$$w1 = \begin{bmatrix} 0.79 & 0.85 & 0.56 & 1.04 & -0.19 & 0.77 & 0.51 \\ 0.42 & 0.95 & 0.55 & 0.85 & 0.53 & 0.37 & 0.73 \\ 0.55 & 1.35 & 0.53 & 0.31 & -0.74 & 0.28 & 0.55 \\ 1.87 & 1.94 & 1.04 & -0.08 & -1.17 & 0.67 & -0.33 \end{bmatrix}$$

and

$$w2 = \begin{bmatrix} 2.36 & 0.55 & 0.18 & 0.90 & 1.77 \end{bmatrix},$$

being, again, w1 the hidden layer weight matrix and w2 the output layer weight matrix, as previously described.

The error and correlation values of the fifth simulation show that this network topology presented the best result and the weights obtained confirm what has already been observed in the previous simulations: coefficients of the hammer weight (W) and hammer drop height (H) variables present numerical superiority to the values of the other coefficients.

Finally, the last simulation was performed using learning rate $\mu=0.5000$ and nno=2 (Figure 6). The analysis metrics indicated in this case the values of MSE=1.3211×10^6 and correlation=0.9433.

Figure 6. Comparison between actual values and ANN outputs ($\mu = 0.5000$ and $nno = 2$).
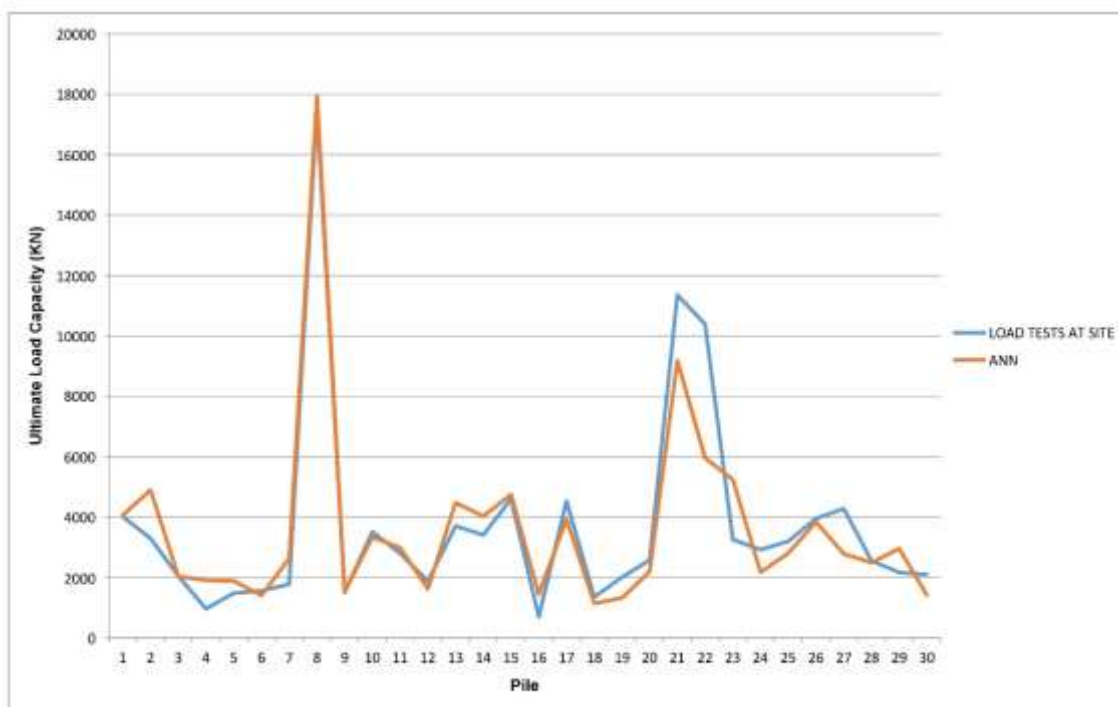
Source: Authors.

In the last simulation performed, it was again realized that for some samples the network fails in the forecast (in this case for samples 21 and 22).

The optimal weights obtained in this simulation were:

$$w1 = \begin{bmatrix} 1.56 & 0.90 & 1.21 & -0.03 & -3.31 & 0.58 & -0,01 \\ 0.92 & 1.93 & 0.77 & 1.30 & 0.07 & 0.22 & 0.56 \end{bmatrix}$$

and

$$w2 = \begin{bmatrix} 2.33 & 2.14 & 1.44 \end{bmatrix},$$

In the sixth and last simulation a fact draws attention. This fact refers to the coefficient value of the variable "permanent penetration of a pile caused by the application of the last hammer blow" which presents, in module, the highest value among the coefficients, but contributes in order to ponder with a negative sign to the main value. Despite the fact exposed, the numerical superiority of the coefficients of the variables hammer weight (W) and hammer drop height (H) remains, which confirms their importance.

It is important to point out that, initially, it has been trained ANN with 8 neurons in the hidden layer and the results were generally satisfactory both in relation to the error and in relation to the correlation. On the other hand, when it has been decreased the number of neurons to 2, the test results were still satisfactory, as shown in the figures. This fact suggests that the approximation of load capacity values is a problem "close to linearity".

When comparing the mean squared errors and correlations, it can be verified that the best result obtained by ANN was when the parameters used were the learning rate $\mu=0.5000$ and nno=8. It is noteworthy that in this simulation correlation was not very high (0.78), but the main objective is the minimization of the mean squared error, and in this case, the study obtained the smallest error (1.4×10^6) when the model was performed without including the modulus of elasticity.

When the information about the modulus of elasticity of the pile was added there was an improvement in the results. The correlation reached 0.96 and the MSE 0.8×10^6 when $\mu=0.9$ and nno=4. This fact highlights the importance of knowing in advance the value of the modulus of elasticity for calculation of load capacity.

In summary, it was noticed that the best result was obtained when using the model with 4 neurons in the hidden layer (nno=4), learning rate $\mu=0.9$ and inclusion of the modulus of elasticity in the input parameters. With this topology, a correlation of 0.96 was obtained between the predicted load capacity values and the actual data, in addition the mean quadratic error was the lowest found in all simulations (0.8×10^6). It was also verified that the hammer drop height obtained, in general, the highest numerical values of weights (values in the second column of w1).

Pessoa (2018) compared the results of five dynamic formulas (Jambu, Danish, Gates, WSDOT, FHWA) with the values of load tests and found WSDOT results as the best prediction, which presented MSE=3.21×10^6 and correlation 0.84. These results reinforce that ANN's estimates (especially when including modulus of elasticity, $\mu=0.9$ and nno=4) are significantly better than such formulas, which although admittedly inaccurate are traditionally used in the geotechnical practice.

As the main proposal of this work is to present a computational model based on neural computing, an algorithm is presented in pseudocode (Table 2) that can be implemented in any programming language, including Excel, in order to enable anyone to use in practice the results presented here.

Table 2. Algorithm in Pseudocode.

Algorithm 1: Neural Model
Inputs: Vector v with the values of hammer weight, hammer drop height, pile weight, pile diameter, permanent penetration of a per blow and modulus of elasticity (All normalized).
2. Multiplication of v by w1 ;
3. Multiplication result apply in sigmoid function
4. Subtract a vector from 1
5. Multiply by w2;
6. Result of multiplication apply in sigmoid function;
7. Undo normalization
8. End

Source: Authors.

4. Conclusion

The major achievement of the work was to get a model which results, considering the values obtained in the metrics of comparison, seem to be very good. In this way, the model shows potential to be adopted as a method of predicting the ultimate load capacity.

As the main objective of this work is to present a computational model based on neural computing, all matrices of synaptic weights were made available, which allows the proposed model to be implemented in any language of programming, so that any user can use it in practice.

Despite the good results obtained by ANN, it is worth mentioning that an important limitation for this type of model was the amount of data available for simulation. We believe that if the database were larger the study could further improve these results. However, the neuronal model presented, even with these limitations, presented encouraging results regarding the prediction of load capacity in foundations.

So, in relation to the results obtained here, future studies should include a refinement of the model, through the expansion of the database used as input values. Also, it would be important to compare the accuracy of the proposed model and that of other prediction methods, such as the empirical and semi-empirical formulas and (mainly) the dynamic formulas (because they are based on the same input parameters).

Besides it, although the results obtained by ANN training are very promising, it is worth investigating, as future studies, simulations using other learning algorithms, such as Momentum and Levemberg Maquart, and comparing them with the Downward Gradient.

References

ABNT, N. B. R. (2010). *Projeto e execução de fundações*. Associação Brasileira de Normas Técnicas, Rio de Janeiro, Brasil.

Amancio, L. B. (2013). *Previsão de Recalques em Fundações Profundas Utilizando Redes Neurais Artificiais do Tipo Perceptron*. Dissertação (Mestrado) - Mestraod em Engenharia Civil: Geotecnia. Centro de Tecnologia. Universidade Federal do Ceará, Fortaleza.

Araújo, C. B. C., Neto, S. A. D. & Anjos, G. J. M. dos. (2015). *Estimativa de Recalque em Estacas Utilizando Redes Neurais Artificiais*. Anais do VII Simpósio Brasileiro de Engenheiros Geotécnicos Jovens.

Azeredo, H. A. (1977). *O Edifício Até Sua Cobertura*. (2nd ed.) Edgard Blücher, São Paulo.

Batista, C. F. B. (2012). *Soluções de Equações Diferenciais Usando Redes Neurais de Múltiplas camadas com os métodos da Descida mais íngreme e Levenberg-Marquardt*. Dissertação (Mestrado). Programa de Pós-graduação em Matemática. Universidade Federal do Pará, Belém.

Benesty, J., Chen, J., Huang, Y., & Cohen, I. (2009). Pearson correlation coefficient. In: *Noise reduction in speech processing*. (pp. 1-4). Springer, Berlin, Heidelberg.

Bowles, J. E. (1996). *Foundation Analysis and Design*. (5th ed.), The McGraw-Hill Companies, Inc., New York.

Cintra, J. C. A. & Aoki, N. (2011). *Fundações por estacas: projeto geotécnico*. Oficina de Textos, São Paulo.

Das, B. M. (2010). *Principles of the Geotechnical Engineering*. (7th ed.), Cengage Learning, Stamford.

Das, B. M. (2011). *Principles of Foundation Engineering*. Seventh Edition.Cengage Learning, Stamford.

Erzin, Y. & Gul, T. O. (2014). The use of neural networks for the prediction of the settlement of one-way footings on cohesionless soils based on standard penetration test. *Neural Computing and Applications*, 24(3–4), 891–900.

Fellenius, B. H. (2020). *Basics of Foundation Design*. British Columbia. <http://www.fellenius.net/papers/401%20The%20Red%20Book,%20Basics%20of%20foundation%20design%202020.pdf>

Hachich, W. C., Falconi, F. F., Saes, J., Frota, R. G. Q., Carvalho, C. S. & Niyama, S. (1998). *Fundações – Teoria e prática*. Ed. Pini, ABMS/ABEF, (2nd. ed.).

Haykin, S. (2001). *Redes Neurais: Princípios e Prática*. (2nd ed.), Bookman, Porto Alegre.

Jayaweera, M. S. R. (2009). *Capacity Estimation of Piles Using Dynamic Methods*. Master of Engineering in Foundation Engineering & Earth Retaining Systems. University of Moratuwa. Sri-Lanka

Kalinli, A., Acar, M. C. & Gündüz, Z. (2011). New approaches to determine the ultimate bearing capacity of shallow foundations based on artificial neural networks and ant colony optimization. *Engineering Geology*, 117(1–2), 29–38.

Khanlari, G. R., Mojtaba, H., Momeni, A.A. & Abdin, Y. (2012). Prediction of shear strength parameters of soils using artificial neural networks and multivariate regression methods. *Engineering Geology*, 131–132, 11–18, 2012.

Lobo, B. O. (2005). *Método de previsão de capacidade de carga de estacas : aplicação dos conceitos de energia do ensaio SPT*. Dissertação (Mestrado). Programa de Pós-Graduação em Engenharia Civil. UFRGS, Porto Alegre .

Padmini, D., Ilamparuthi, K. &Sudheer, K. P. (2008). Ultimate bearing capacity prediction of shallow foundations on cohesionless soils using neurofuzzy models. *Computers and Geotechnics*, v. 35, n. 1, p. 33–46.

Pereira, A. S., Shitsuka, D. M., Parreira, F. J., & Shitsuka, R. (2018). *Metodologia da pesquisa científica*. [eBook]. Santa Maria. Ed. UAB / NTE / UFSM. https://repositorio.ufsm.br/bitstream/handle/1/15824/Lic_Computacao_Metodologia-Pesquisa-Cientifica.pdf?sequence=1.

Pessoa, A. D. (2018). *Modelo Neuronal para Previsão de Capacidade de Carga em Fundações Profundas*. Universidade Federal do Maranhão, São Luis.

SCAC. (2013). *Case: conjunto residencial no Rio de Janeiro*. <https://issuu.com/scacengenharia/docs/scac_case_conj_residencial_rj>

Shanazari, H. & Tutunchian, M. A. (2012). Prediction of ultimate bearing capacity of shallow foundations on cohesionless soils: An evolutionary approach. *KSCE Journal of Civil Engineering*, 16(6), 950–957.

Silva, I. N., Spatti, D. & Flauzino, R. (2016). *Redes Neurais Artificiais para Engenharia e Ciências Aplicadas: Curso Prático*. (2nd ed.), São Paulo. Artliber Editora.

Tian, H. & Shang, Z. (2006). Artificial neural network as a classification method of mice by their calls. *Ultrasonics*, 44, e275--e278.

Velloso, D. A. & Lopes, F. de R. (2011). *Fundações: critérios de projeto, investigação do subsolo, fundações superficiais, fundações profundas*. Oficina de Textos, São Paulo.

Vesic, A. S. (1963). Bearing Capacity of Deep Foundations in Sand. National Academy of Sciences, *Highway Research Board*, Report No. 39, Washington D.C. pp. 112-153.

Willmott, C. J. & Matsuura, K. (2005). Advantages of the mean absolute error (MAE) over the root mean square error (RMSE) in assessing average model performance. *Clim Res*. 30(1):79–82.

Yan, H., Jiang, Y., Zheng, J., Peng, C. & Li, Q. (2006). A multilayer perceptron-based medical decision support system for heart disease diagnosis. *Expert Systems with Applications*, 30(2), 272–281.

Zanella,   L.   C.   H.   (2011).   *Metodologia   de   Pesquisa.*   (2nd   ed.).
<http://arquivos.eadadm.ufsc.br/EaDADM/UAB_2014_2/Modulo_1/Metodologia/material_didatico/Livro texto Metodologia da Pesquisa.pdf>